Compositional Effect on the Two-Stage Enthalpy Relaxation of Metal-Metalloid Amorphous Alloys upon Annealing*

Akihisa Inoue, H. S. Chen**, Tsuyoshi Masumoto and S. A. Ajuria***

The Research Institute for Iron, Steel and Other Metals

(Received January 23, 1985)

Synopsis

The anneal-induced enthalpy relaxation behavior was examined calorimetrically for amorphous alloys of Fe-P, Fe-B, Ni-P, Ni-B, Fe-Ni-P, Fe-Ni-B and Fe-Ni-Co-P systems. When the alloys annealed at temperatures below T_g are heated, an excess endothermic reaction (enthalpy relaxation) occurs above the annealing temperature, T_a. The magnitudes of $\Delta C_{p,endo}$ and ΔH_{endo} for the alloys of Fe-P, Fe-B, Ni-P and Ni-B containing only one metallic element first increase gradually with rising T_a and then rapidly at temperatures just below T_g, while their changes as a function of T_a for the alloys containing more than two metallic elements show a distinct two-stage splitting; a low-temperature peak at about T_g-200 K and a high-temperature peak just below T_g. From the result that the addition of the second metallic element causes the two-stage splitting of the $\Delta C_{p,endo}(T_a)$, it has been proposed that the low-temperature endothermic peak is attributed to short-range rearrangement of metal-metal atoms with weak bonding nature and the high-temperature peak to the long-range cooperative regrouping of metal-metalloid atoms which are composed of the skeleton structure in the metal-metalloid amorphous alloys. The mechanism for the appearance of the two-stage enthalpy relaxation has been investigated by the concept of two-stage distributions of relaxation times proposed previously by the present authors and the distinct two-stage splitting has been interpreted to be generated by the distinguishable difference in the ease of atomic rearrangement between metal-metal and metal-metalloid.

---

* The 1777th report of the Research Institute for Iron, Steel and Other Metals.

** ATT Bell Laboratories, Murray Hill, New Jersey 07974, U.S.A.

*** Department of Materials Science and Engineering, Massachusetts Institute of Technology, Cambridge, Massachusetts 02139, U.S.A.

I. Introduction

It is very important for thermodynamically nonequilibrium amorphous alloys to clarify quantitatively the structural relaxation behavior resulting from annealing at temperatures well below the glass transition temperature (T_g) or crystallization temperature (T_x), because relaxation causes significant changes in physical, mechanical and chemical properties such as ferromagnetic Curie temperature[1-4], superconducting critical temperature[5-9], electrical resistance[10-13], Young's modulus[14-16], internal friction[17-22], fracture strain[23-25], and anodic current density[26,27] etc. To this date, much information on the structural relaxation of amorphous alloys has been presented[28,29] which enables us to interpret semi-quantitatively anneal-induced structural changes. Among the previous publications, the two-stage distribution of enthalpy relaxation found most recently by Inoue et al. for the metal-metalloid alloys of (Fe, Co, Ni)-Si-B[30], Fe-Ni-P [31] and Fe-Ni-B[31] as well as the metal-metal alloys of Cu-Zr-Fe[32] and Cu-Zr-Ni[32] is thought to be one of the most important in the immutable interpretation on the structural relaxation behavior of an amorphous alloy. That is, the magnitude of an excess endothermic reaction (enthalpy relaxation), which occurs upon heating the sample annealed at temperatures below T_g, as a function of annealing temperature shows clearly two distinct stages; a low-temperature peak at about T_g - 200 K and a high-temperature peak just below T_g. It has been interpreted that the low-temperature endothermic reaction is due to local and medium range rearrangements of metal atoms and the high-temperature reaction to the long-range cooperative regroupings of metal and metalloid atoms. Furthermore, the interpretation of the appearance of the two-stage enthalpy relaxation is based on the new concept of a two-stage distribution in relaxation times (e.g., two-stage glass transitions). The concept of the local and medium rearrangements with shorter relaxation times due to metal atoms is quite significant in the understanding of the effect of structural relaxation on various kinds of properties for amorphous alloys subjected to low-temperature annealing, because the relaxation time is shorter by many orders of magnitude than that required for the cooperative relaxation due to metal-metalloid atoms responsible for the commonly observed glass transition. This paper intends (1) to give an outline of the two-stage enthalpy relaxation phenomenon for $(Fe_{0.5}Ni_{0.5})_{83}P_{17}$ and $(Fe_{0.5}Ni_{0.5})_{83}B_{17}$ amorphous alloys[31] found previously by the present authors, (2) to present the compositional effect on the anneal-induced two-stage enthalpy relaxation behavior of (Fe, Ni)-P, (Fe, Ni)-B and (Fe, Co, Ni)-P amor-

phous alloys, and (3) to reconfirm the invariability of the concept of the two-stage enthalpy relaxation in the whole amorphous alloys.

II. Experimental Procedures

Ribbon samples of $(Fe_{1-x}Ni_x)_{83}P_{17}$, $(Fe_{1-x}Ni_x)_{83}B_{17}$ (x=0, 0.25, 0.50, 0.75 and 1.0), $(Fe_{0.5}Ni_{0.5})_{100-y}P_y$, $(Fe_{0.5}Ni_{0.5})_{100-y}B_y$ (y=15, 17, 20 and 25) and $(Fe_{0.33}Ni_{0.33}Co_{0.34})_{83}P_{17}$ alloys, typically 20 μm in thickness and 1.5 mm in width, were prepared by a single-roller melt spinning method and confirmed to be amorphous by conventional X-ray diffraction using Cu-Kα radiation in combination with an X-ray monochromator. The subscripts are assumed to be those of the unalloyed pure elements since the difference between nominal and chemically analyzed compositions was less than 0.20 wt% for phosphorus, 0.12 wt% for boron and 0.66 wt% for nickel. The apparent specific heat, C_p, was measured with a differential scanning calorimeter (Perkin Elmer DSC-II). Care was taken to reduce thermal drift by prewarming the calorimeter for at least 5 h in the temperature range of interest. The accuracy of the data was approximately 0.8 J/mol-K for the absolute C_p values, but was better than 0.2 J/mol-K for the relative C_p and ΔC_p measurements.

The as-quenched samples were subjected to annealing treatments at various temperatures below T_g (T_a=350 - 600 K) for different periods of time (t_a=1 - 200 h). Short-time anneals ($t_a \leq 13$ h) were performed directly inside the calorimeter while long-time anneals (14 - 200 h) were performed in a well-controlled furnace after placing the encapsulated samples in a vacuum-sealed quartz tube.

Following the annealing treatment, the sample was thermally scanned at 40 K/min from 320 K to T_g to determine the $C_{p,q}$ of the as-quenched or the $C_{p,a}$ of the annealed sample. It was then cooled to 320 K, and reheated immediately to obtain the $C_{p,s}$ data of the "reference" sample (i.e., the preconditioned sample without further low-temperature annealing). This test procedure is essential in order to eliminate any possible error that might result from the drift in the calorimeter. The change in the calorimetric behavior with annealing was used in monitoring the structural relaxation processes.

III. Results

1. $C_p(T)$ and $\Delta C_p(T)$ behaviors of as-quenched and annealed samples

As examples, Figs. 1 and 2 show the changes in the thermograms (a) and the temperature dependence of the configuration enthalpy $\Delta H_\sigma(T)$ (b)

of an amorphous $(Fe_{0.5}Ni_{0.5})_{83}P_{17}$ alloy subjected to isochronal (t_a=13 h) and isothermal (T_a=475 K) anneals. Here the temperature dependence of the vibrational specific heat, $C_{p,\nu}$, in Fig. 1 (a) and Fig. 2 (a) is obtained by linear extrapolation of the $C_{p,s}$ curve in the low temperature region $T \lesssim 450$ K, which is independent on the thermal history and arises from purely thermal vibrations, and is expressed by

$$C_{p,\nu} = 27.9 + 7.0\times10^{-3}(T - 530) \quad \text{J/mol-K.} \tag{1}$$

Also the configuration enthalpy is taken to be the reference with ΔH_σ (675K) = 0, and the relaxed configurational enthalpy $\Delta H_\sigma(T)$ is evaluated by

$$\Delta H_\sigma(T) = \int_{675}^{T} (C_{p,a} - C_{p,\nu})dT. \tag{2}$$

The C_p value of the as-quenched phase is about 26 J/mol-K near room temperature. As the temperature rises, the $C_{p,q}$ value begins to decrease, indicative of structural relaxation at about 375 K, exhibits two minimum peaks at about 480 K and about 600 K in the range below 650 K, then increases rapidly in the region of glass transition and reaches an equilibrium supercooled liquid value of about 43.7 J/mol-K around 680 K. It can be seen that the $C_{p,s}$ value near room temperature is consistently lower by about 0.1 - 0.2 J/mol-K than the $C_{p,q}$ value. The small difference in C_p is attributed to the anneal-induced changes in physical, mechanical and chemical properties. The heating curve of the annealed sample, $C_{p,a}$, shows a $C_p(T)$ behavior which closely follows the specific

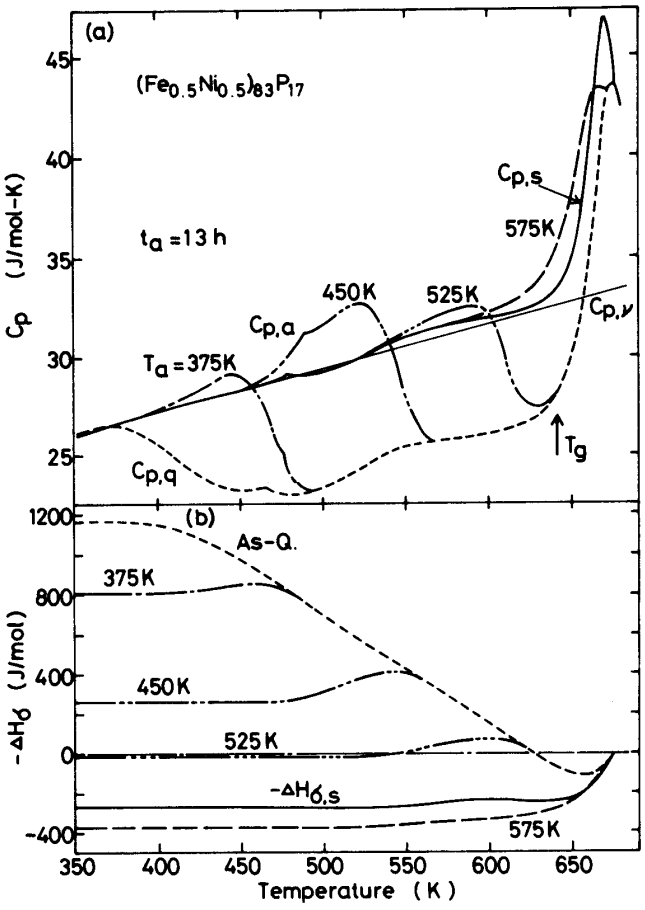

Fig. 1 (a) The endothermic peak of an amorphous $(Fe_{0.5}Ni_{0.5})_{83}P_{17}$ alloy subjected to anneals for 13 h at various temperatures ranging from 375 to 575 K. (b) The change in the configuration enthalpy $\Delta H_\sigma(T)$ corresponding to the appearance of the endothermic peak, where ΔH_σ(675K) is set to zero.

heat curve of the reference sample, $C_{p,s}$, up to each T_a, and then exhibits an excess endothermic peak relative to the reference sample before merging with that of the as-quenched sample at a temperature below T_g=645 K, where T_g is defined as the point of inflection in the $C_p(T)$ curve.

The other significant features obtained from the data of Figs. 1 and 2 are summarized as follows: (1) The sample annealed at T_a shows an excess endothermic reaction beginning at T_a. (2) The temperature ($\simeq T_a$) where the excess endothermic peak begins to rise is independent on the annealing time. (3) The temperature of the endothermic peak increases linearly with the logarithm of the time ($\ell n\ t_a$)[31]. (4) The excess endothermic peak is reversible while the exothermic broad peak is irreversible and the $C_{p,a}(T)$ curves of the annealed samples couple the reversible endothermic and irreversible exothermic reaction[31]. (5) If the annealing is performed at temperatures well below T_g ($T_a \leq$ 550 K), it does not affect the glass transition process. This is indicated by the close overlap of $C_p(T)$ curves for the annealed and unannealed samples at temperatures below T_g. (6) The change in the magnitude of the endothermic peak with T_a is not monotonous and can be divided into two stages having the peak at $T_a \simeq$ 450 K and $T_a \simeq T_g$, indicating the appearance of the two-stage enthalpy relaxation (see also Figs. 3 and 4). (7) The configurational enthalpy curve falls progressively with T_a and t_a, indicating that the low-temperature anneals

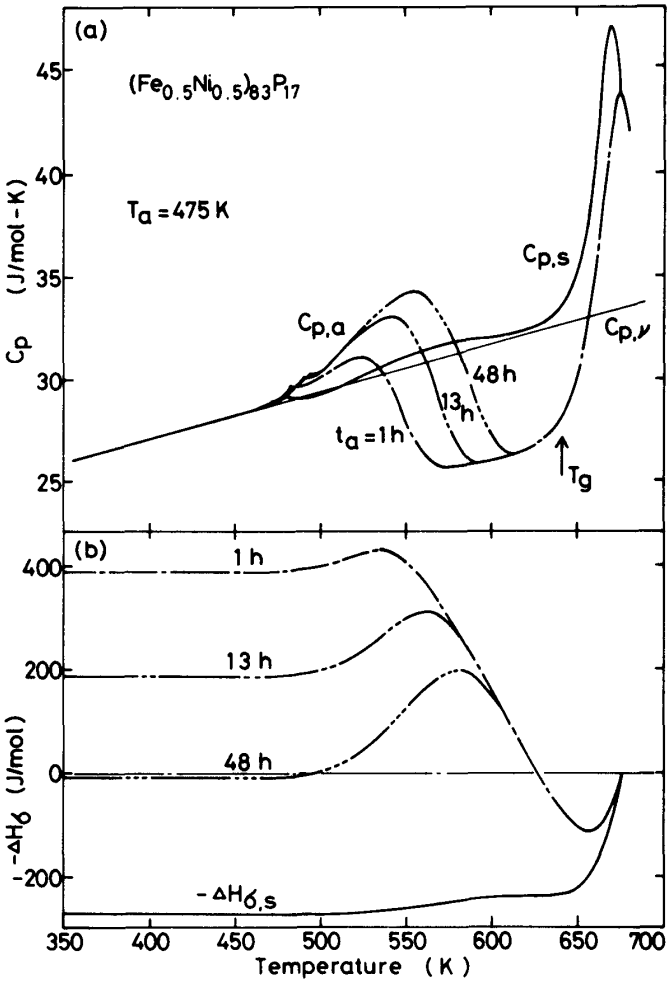

Fig. 2 (a) The endothermic peak of an amorphous $(Fe_{0.5}Ni_{0.5})_{83}P_{17}$ alloy subjected to anneals at 475 K for various periods from 1 to 48 h. (b) The change in the configuration enthalpy $\Delta H_\sigma(T)$ corresponding to the appearance of the endothermic peak, where ΔH_σ(675K) is set to zero.

result in a stabilization of the amorphous structure and a lowering of fictive temperature. (8) With rising temperature, the $\Delta H_{\sigma}(T)$ of the annealed sample approaches the reference values $\Delta H_{\sigma,s}(T)$ and merges with it before the complete transition from amorphous solid to supercooled liquid, showing that it is possible to recover completely the initial structure of the amorphous alloy without reheating above T_g. This feature differs significantly from the common phenomenon of glass transition[33-35].

Quite similar $C_{p,a}(T)$ curves as a function of T_a and/or t_a were recognized for all the amorphous alloys containing two or more metallic elements, i.e., with the exception of $Fe_{83}P_{17}$, $Fe_{83}B_{17}$, $Ni_{83}P_{17}$ and $Ni_{83}B_{17}$.

2. Changes in $\Delta C_{p,endo}$ and $\Delta H_{\sigma,endo}$ with T_a and t_a

In order to reconfirm the two-stage change in the magnitude of the endothermic peak with T_a, the temperature dependence of the differences in C_p between annealed (T_a=350 - 600 K, t_a=1, 3, 13, 48 h) and the reference states, [$\Delta C_{p,endo} = C_{p,a}(T) - C_{p,s}(T)$] is shown in Fig. 3 for $(Fe_{0.5}Ni_{0.5})_{83}P_{17}$ and Fig. 4 for $(Fe_{0.5}Ni_{0.5})_{83}B_{17}$. One can see clearly that the change in the magnitude of the $\Delta C_{p,endo}$ with T_a shows two separatable maxima which peak respectively at T_a=450 K and T_a=575 - 600 K for the Fe-Ni-P samples and at T_a=550 K and T_a=600 - 625 K for the Fe-Ni-B samples, indicating that the anneal-induced enthalpy relaxation occurs by two separatable mechanisms.

The changes in the maximum differential specific heat, $\Delta C_{p,max} = C_{p,a} - C_{p,s}$, and the enthalpy relaxation, $\Delta H_{\sigma,endo}$, during annealing for different periods (t_a) as a function of T_a are shown in Fig. 5 for $(Fe_{0.5}Ni_{0.5})_{83}P_{17}$ and Fig. 6 for $(Fe_{0.5}Ni_{0.5})_{83}B_{17}$, where

$$\Delta H_{\sigma,endo}(T_a,t_a) = \int \Delta C_p(T) = \int (C_{p,a} - C_{p,s})dT \quad \text{at } \Delta C_p \geq 0. \quad (3)$$

With increasing T_a, both the values $\Delta C_{p,max}$ and $\Delta H_{\sigma,endo}$ increase at first, show maximum values at about 450 K for the Fe-Ni-P alloy and at about 525 K for the Fe-Ni-B alloy, and then decrease significantly in the range from 450 to 550 K for the former alloy and from 525 to 575 K for the latter alloy followed by a rapid increase at temperatures slightly below T_g. Similar two-stage changes in the $\Delta C_{p,endo}$ and $\Delta H_{\sigma,endo}$ with T_a have been recognized for all the metal-metal-metalloid amorphous alloys consisting of two kinds of metallic elements as exemplified by $(Fe_{0.5}Ni_{0.5})_{75}Si_{10}B_{15}$ in Fig. 7[30]. The distinct splitting of the peaks of the $\Delta C_{p,max}(t_a)$ and $\Delta H_{\sigma,endo}(t_a)$ as a function of T_a indicates clearly that the enthalpy relaxation of the amorphous alloys on annealing occurs by two distinguishable mechanisms. The rapid increases in the $\Delta C_{p,max}$ and $\Delta H_{\sigma,endo}$ at temperatures above 550 K for the

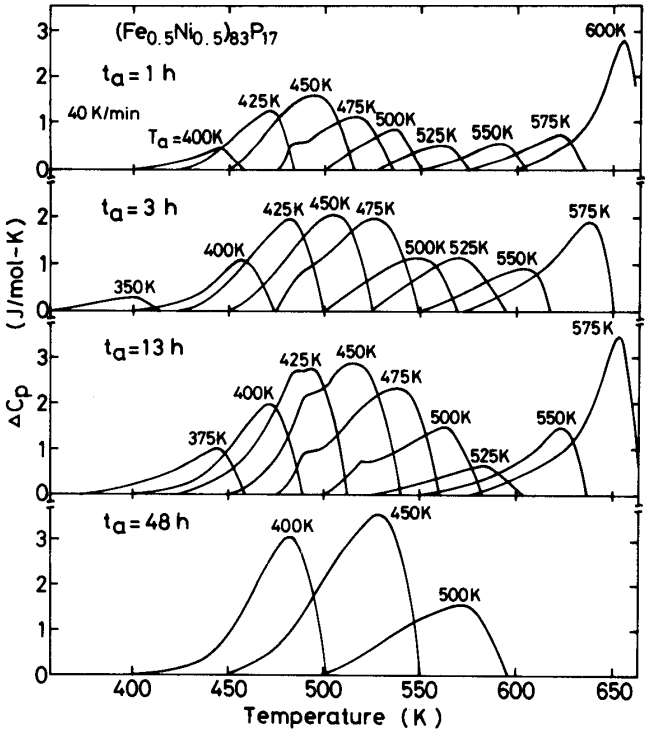

Fig. 3 The differential specific heat, $\Delta C_p(T)$, between the reference and annealed samples for an amorphous $(Fe_{0.5}Ni_{0.5})_{83}P_{17}$ alloy subjected to anneals at various temperatures ranging from 400 to 600 K for different periods from 1 to 48 h.

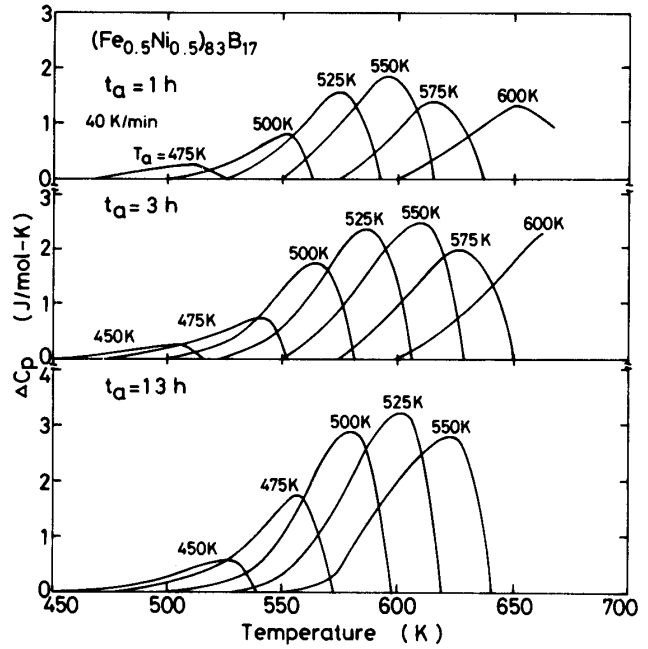

Fig. 4 The differential specific heat, $\Delta C_p(T)$, between the reference and annealed samples for an amorphous $(Fe_{0.5}Ni_{0.5})_{83}B_{17}$ alloy subjected to anneals at various temperatures ranging from 450 to 600 K for different periods from 1 to 13 h.

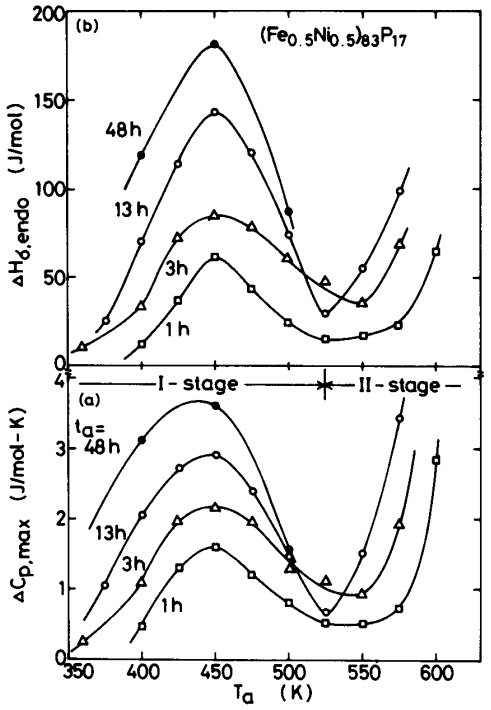

Fig. 5 The variations of the maximum differential specific heat, $\Delta C_{p,max}$(a) and the enthalpy relaxation $\Delta H_{\sigma,endo}$(b) as a function of annealing temperature for an amorphous $(Fe_{0.5}Ni_{0.5})_{83}P_{17}$ alloy subjected to anneals for different periods from 1 to 48 h.

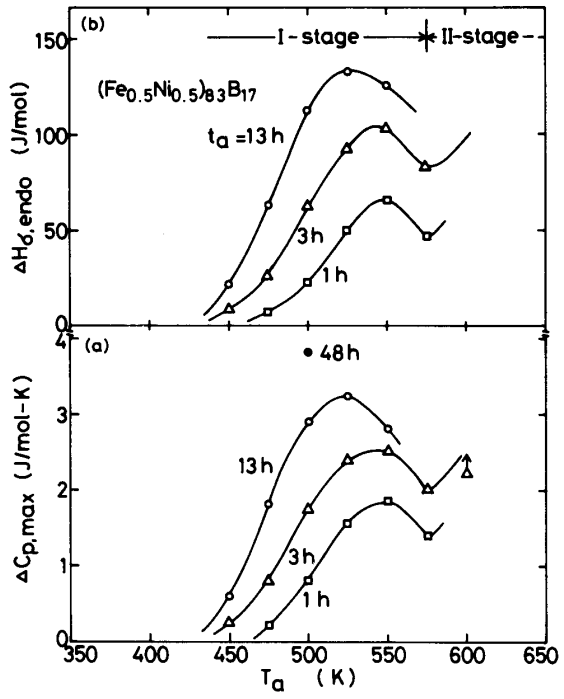

Fig. 6 The variations of the maximum differential specific heat, $\Delta C_{p,max}$(a) and the enthalpy relaxation $\Delta H_{\sigma,endo}$(b) as a function of annealing temperature for an amorphous $(Fe_{0.5}Ni_{0.5})_{83}B_{17}$ alloy subjected to anneals for different periods from 1 to 48 h.

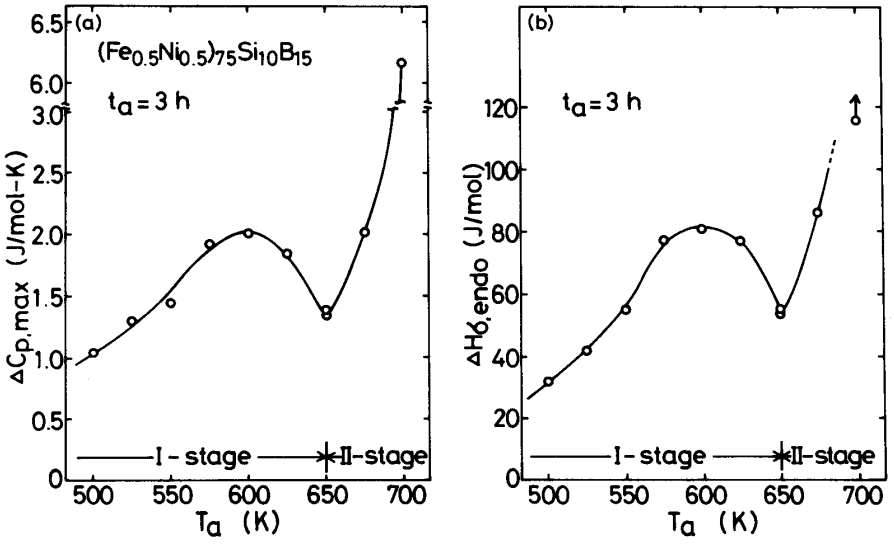

Fig. 7 The variations of the maximum differential specific heat, $\Delta C_{p,max}$ (a) and the enthalpy relaxation $\Delta H_{\sigma,endo}$ (b) as a function of annealing temperature for an amorphous $(Fe_{0.5}Ni_{0.5})_{75}Si_{10}B_{15}$ alloy subjected to anneals for different periods from 1 to 48 h.

Fe-Ni-P alloy and above 575 K for the Fe-Ni-B alloy are interpreted to correspond to the common glass transition phenomenon. Here it is worthy to point out that the $\Delta C_{p,max}(T_a)$ and $\Delta H_{\sigma,endo}(T_a)$ behaviors of the annealed samples are similar to the exothermic $\Delta C_p(T)$ behavior of the as-quenched samples (Fig. 8) regarding the appearance of the two-stage relaxation and their peak temperatures. The similarity suggests that the reaction mechanisms at each stage for the irreversible and the reversible structural relaxations are similar.

Furthermore, the two-stage splitting of the endothermic peak is seen for all the metal-metal-metalloid amorphous samples even after pre-annealing for 1 min at a temperature near T_g (640 K) as exemplified by $(Fe_{0.5}Ni_{0.5})_{83}P_{17}$ in Fig. 9. The magnitude of the $\Delta C_{p,endo}$ peak of the pre-annealed samples, however, is smaller by about 40 % than that of the as-quenched samples and the annealing temperature at which the $\Delta C_{p,max}$ for the first-stage reaction exhibits a maximum value increases from ≃450 K for the as-quenched sample to ≃475 K for the pre-annealed sample. Such differences in the

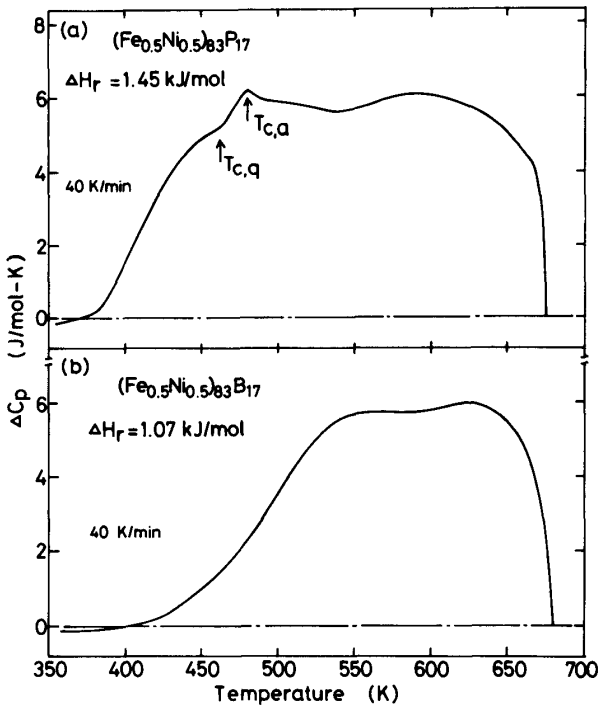

Fig. 8 Difference in the specific heat between the as-quenched and annealed state, $\Delta C_{p,exo}$, vs. temperature for amorphous $(Fe_{0.5}Ni_{0.5})_{83}P_{17}$ and $(Fe_{0.5}Ni_{0.5})_{83}B_{17}$ alloys.

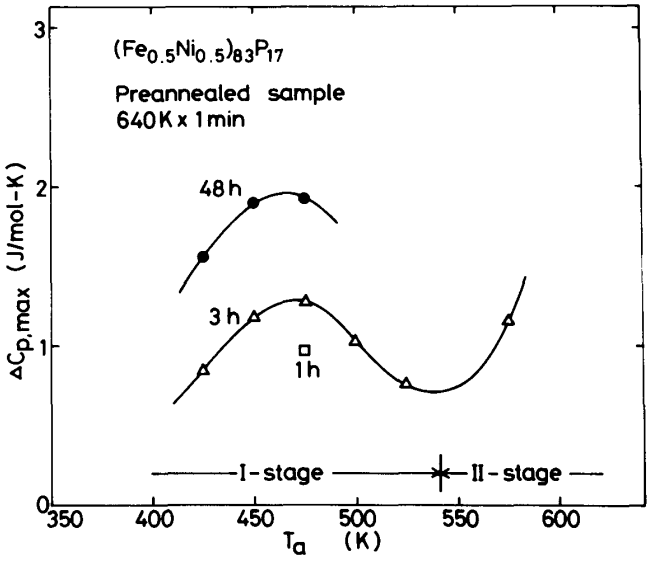

Fig. 9 The variation of the maximum differential specific heat, $\Delta C_{p,max}$, as a function of annealing temperature for an amorphous $(Fe_{0.5}Ni_{0.5})_{83}P_{17}$ alloy subjected to anneals for 3 and 48 h at various temperatures after pre-annealing for 1 min at 640 K.

$\Delta C_{p,endo}$ peak behavior between the as-quenched and the pre-annealed samples have also been recognized for $Pd_{48}Ni_{32}P_{20}$[36].

3. Effect of metal composition on the $\Delta C_{p,max}(T_a)$ and $\Delta H_{\sigma,endo}(T_a)$ behavior

As presented in the previous section, the anneal-induced enthalpy relaxation as a function of T_a for $(Fe_{0.5}Ni_{0.5})_{83}P_{17}$ and $(Fe_{0.5}Ni_{0.5})_{83}B_{17}$ amorphous alloys occurs by two distinguishable processes. In this section, the effect of the ratio of iron to nickel on the two-stage relaxation behavior is analyzed for $(Fe\text{-}Ni)_{83}P_{17}$ amorphous alloys and the $\Delta C_{p,max}$ and $\Delta H_{\sigma,endo}$ values as a function of T_a are shown in Fig. 10 for Ni/(Fe+Ni) = 0.25 and 0.50 and in Fig. 11 for Ni/(Fe+Ni) = 0.50 and 0.75. Additionally, Fig. 12 shows the changes in the maximum $\Delta C_{p,max}$ and $\Delta H_{\sigma,endo}$ values as a function of Ni/(Fe+Ni) for $(Fe\text{-}Ni)_{83}P_{17}$ alloys. The features of these figures may be summarized as follows; (1) the changes of the $\Delta C_{p,max}(T_a)$ and $\Delta H_{\sigma,endo}(T_a)$ are divided into two distinguishable stages, (2) the values of $\Delta C_{p,max}$ and $\Delta H_{\sigma,endo}$ are greatest at Ni/(Fe+Ni) $\simeq$ 0.4 and decrease with deviation from the ratio Ni/(Fe+Ni) = 0.4, (3) the peak temperature of the low-temperature endothermic reaction tends to lower with increasing nickel content, e.g., 450 - 475 K at Ni/(Fe+Ni) = 0.25, about 450 K at Ni/(Fe+Ni) = 0.50 and 425 - 450 K at Ni/(Fe+Ni) = 0.75, (4) the peak temperature of the high-temperature reaction tends to rise with T_g and/or T_x, even though not enough data is available due to the high thermal instability of the amorphous alloys at temperatures near T_g.

Figure 13 shows the effect of the third metallic element (cobalt) on the $\Delta C_{p,endo}(T_a)$ and $\Delta H_{\sigma,endo}(T_a)$ of $(Fe_{0.5}Ni_{0.5})_{83}P_{17}$ amorphous alloy. It is surprising that the $\Delta C_{p,max}$ and $\Delta H_{\sigma,endo}$ values of the first-stage reaction for $(Fe_{0.33}Ni_{0.33}Co_{0.34})_{83}P_{17}$ alloy are larger by about 44 % than those of $(Fe_{0.5}Ni_{0.5})_{83}P_{17}$ alloy. This indicates that the multiplication of the mother metallic components results in a significant increase in the anneal-induced structural relaxation at low temperatures. Figure 14 shows the changes in $\Delta C_{p,max}$ and $\Delta H_{\sigma,endo}$ as a function of T_a for binary $Fe_{83}B_{17}$ amorphous alloy together with the data of $(Fe_{0.5}Ni_{0.5})_{83}B_{17}$. The first stage peak of $\Delta C_{p,max}(T_a)$ and $\Delta H_{\sigma,endo}(T_a)$ disappears for the Fe-B alloy, indicating that the anneal-induced structural relaxation for $Fe_{83}B_{17}$ binary alloy occurs by a single-stage mechanism. From the above-described results, the effects of the metallic composition on the two-stage relaxation behaviors for $(Fe\text{-}Ni)_{83}P_{17}$ amorphous alloy may be summarized as follows: (1) The peak height of the first-stage reaction, $\Delta C_{p,max}$, exhibits a maximum value in the vicinity of Ni/(Fe+Ni) $\simeq$ 0.5, i.e., the low-temperature

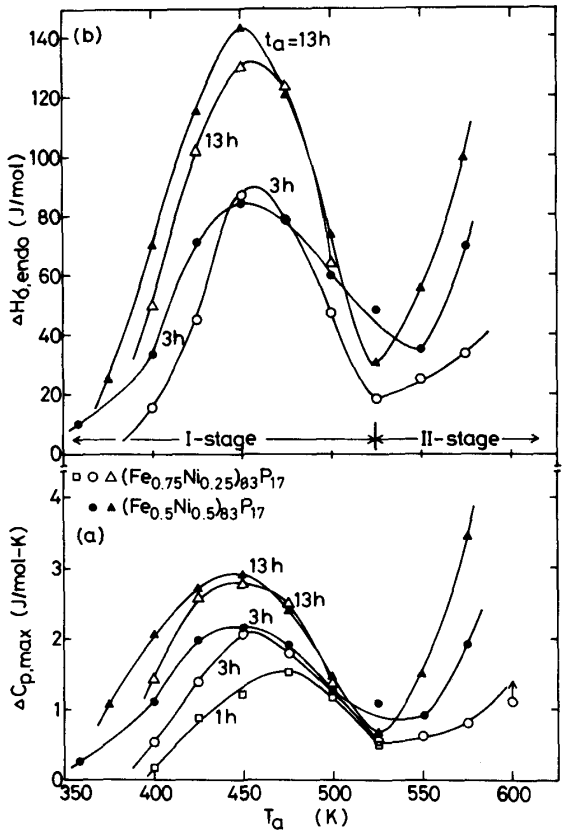

Fig. 10

The variations of the maximum differential specific heat, $\Delta C_{p,max}$, (a) and the enthalpy relaxation, $\Delta H_{\sigma,endo}$ (b) as a function of annealing temperature for an amorphous $(Fe_{0.75}Ni_{0.25})_{83}P_{17}$ alloy subjected to anneals for different periods from 1 to 13 h. The data for an amorphous $(Fe_{0.5}Ni_{0.5})_{83}P_{17}$ alloy are also shown for comparison.

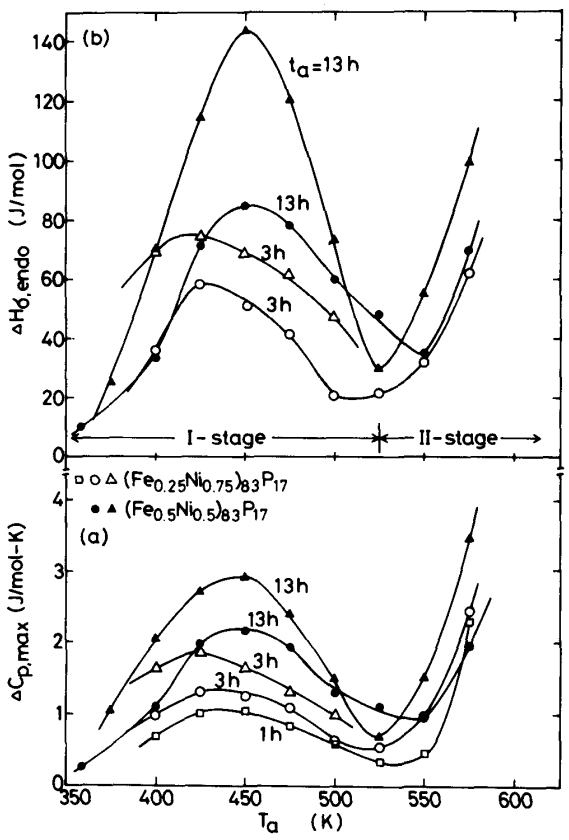

Fig. 11

The variations of the maximum differential specific heat, $\Delta C_{p,max}$ (a) and the enthalpy relaxation, $\Delta H_{\sigma,endo}$ (b) as a function of annealing temperature for an amorphous $(Fe_{0.25}Ni_{0.75})_{83}P_{17}$ alloy subjected to anneals for different periods from 1 to 13 h. The data for an amorphous $(Fe_{0.5}Ni_{0.5})_{83}P_{17}$ alloy are also shown for comparison.

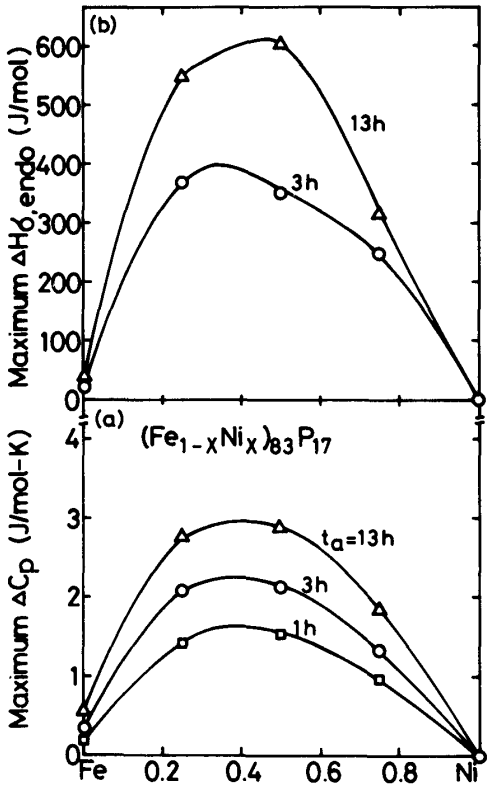

Fig. 12

The composition dependence of the maximum differential specific heat, $\Delta C_{p,max}$ (a) and the enthalpy relaxation, $\Delta H_{\sigma,endo}$ (b) for amorphous $(Fe\text{-}Ni)_{83}P_{17}$ alloys subjected to anneals for different periods from 1 to 13 h at various temperatures ranging from 360 to 600 K.

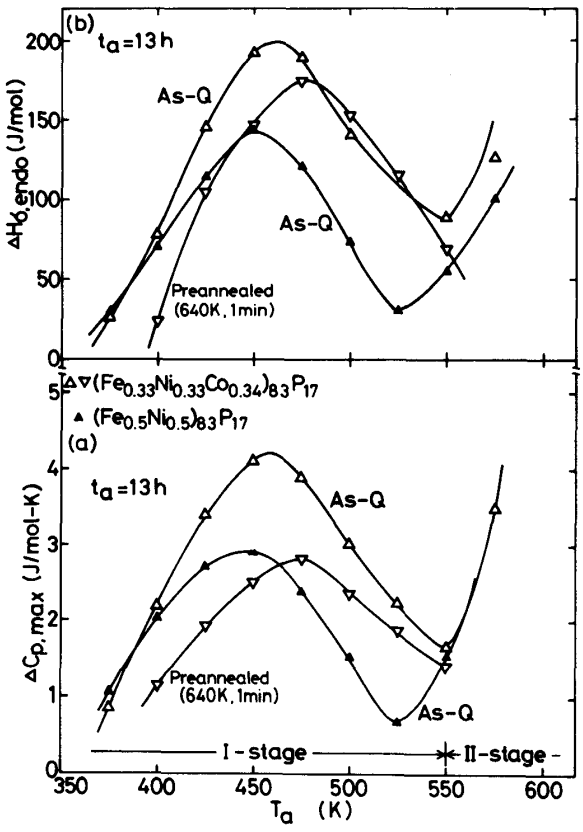

Fig. 13

The variations of the maximum differential specific heat, $\Delta C_{p,max}$ (a) and the enthalpy relaxation, $\Delta H_{\sigma,endo}$ (b) as a function of annealing temperature for an amorphous $(Fe_{0.33}Ni_{0.33}Co_{0.34})_{83}P_{17}$ alloy subjected to anneals for 13 h after melt-quenching or pre-annealing for 1 min at 640 K. The data for an amorphous $(Fe_{0.5}Ni_{0.5})_{83}P_{17}$ alloy are also shown for comparison.

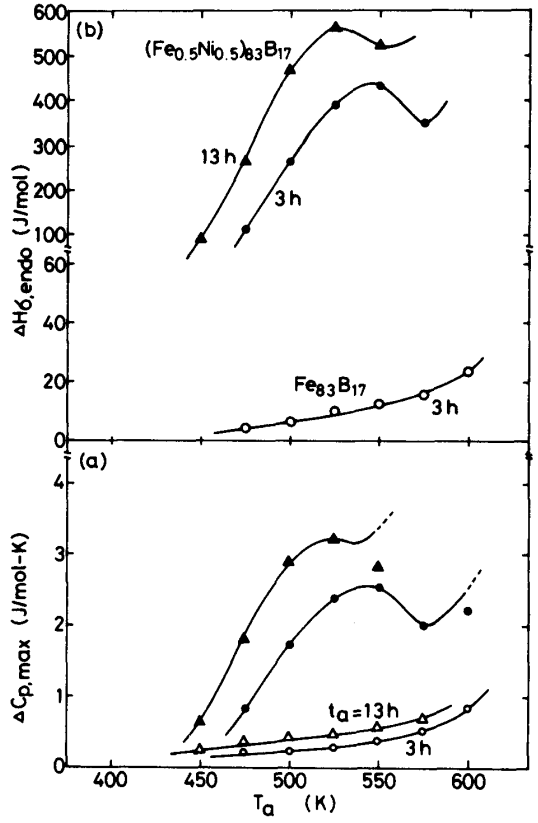

Fig. 14

The variations of the maximum differential specific heat, $\Delta C_{p,max}$ (a) and the enthalpy relaxation, $\Delta H_{\sigma,endo}$ (b) as a function of annealing temperature for an amorphous $Fe_{83}B_{17}$ alloy subjected to anneals for 3 and 13 h. The data for an amorphous $(Fe_{0.5}Ni_{0.5})_{83}B_{17}$ alloy are also shown for comparison.

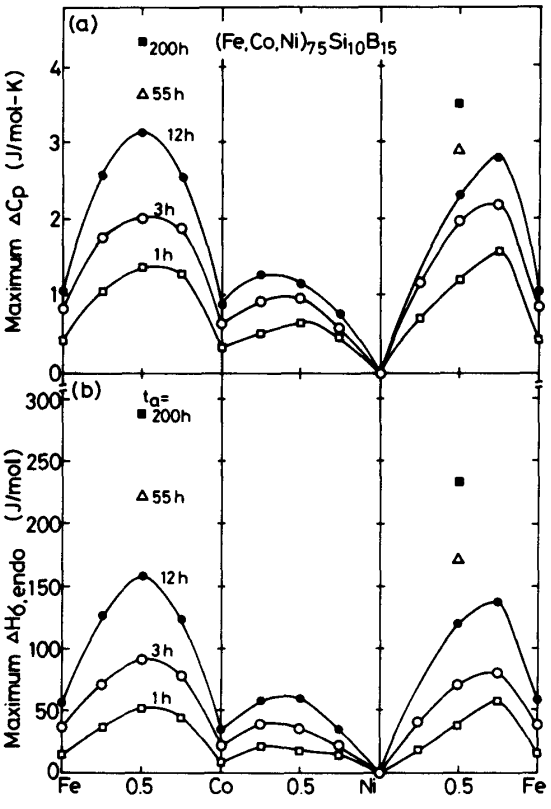

Fig. 15

The composition dependences of the maximum differential specific heat, $\Delta C_{p,max}$ (a) and the enthalpy relaxation $\Delta H_{\sigma,endo}$ (b) for amorphous $(Fe_{1-x}Ni_x)_{75}Si_{10}B_{15}$, $(Ni_{1-x}Co_x)_{75}Si_{10}B_{15}$ and $(Co_{1-x}Fe_x)_{75}Si_{10}B_{15}$ (x=0, 0.25, 0.50, 0.75, 1.0) alloys subjected to anneals at 600 K for different periods from 1 to 200 h.

relaxation becomes easy with an increase in the entropy of mixing of the metallic components. (2) While the first-stage reaction is enhanced significantly by the multiplication of metallic components, the elimination of iron or nickel results in a disappearance of the first-stage reaction. From these results, it is concluded that the first-stage reaction corresponds to the relaxation which occurs by the short-range rearrangement of metallic atoms and the second-stage reaction to one by the long-range rearrangement of metal and metalloid atoms. A similar change in the low-temperature endothermic reaction with metallic component has also been observed[30] for the alloy series of $(Fe, Co)_{75}Si_{10}B_{15}$, $(Fe, Ni)_{75}Si_{10}B_{15}$ and $(Co, Ni)_{75}Si_{10}B_{15}$ (Fig. 15).

4. Effect of metalloid content on the $\Delta C_{p,endo}(T_a)$ and $\Delta H_{\sigma,endo}(T_a)$ behavior

Figure 16 shows the changes in $\Delta C_{p,max}(T_a)$ and $\Delta H_{\sigma,endo}(T_a)$ for $(Fe_{0.5}Ni_{0.5})_{100-x}B_x$ amorphous alloys with boron content. The low-temperature endothermic reaction is greatest at 17 %B and decreases with displacement from 17 %B. In particular, the increase in boron content results in a remarkable suppression of the low-temperature reaction and the magnitude of the low-temperature peak at 25 %B is only about one third of that at 17 %B. Additionally, the annealing temperature leading to the maximum low-temperature reaction rises with increasing boron content from 520 K at 15 %B to 565 K at 25 %B. Thus, the low-temperature endothermic reaction becomes easier with decreasing boron content, but the total amount of structural relaxation appears to show a maximum value in the vicinity of a eutectic composition (≈17

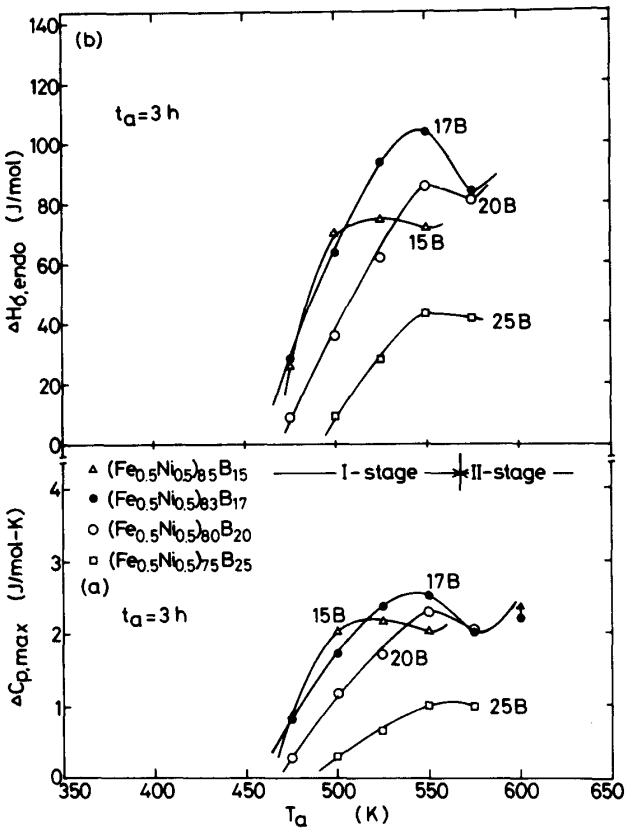

Fig. 16 The variations of the maximum differential specific heat, $\Delta C_{p,max}$ (a) and the enthalpy relaxation, $\Delta H_{\sigma,endo}$ (b) as a function of annealing temperature for amorphous $(Fe_{0.5}Ni_{0.5})_{100-x}B_x$ (x≈ 15, 17, 20, 25) alloys subjected to anneals for 3 h.

%B) and decreases significantly when approaching the stoichiometric compound composition M_3B. Considering the previous results[37-39] that the mechanical strengths of hardness and Young's modulus etc., which are thought to reflect the bonding force of the constituent atoms, increase significantly with increasing boron content, one can notice a tendency that the stronger the bonding force of the constituent atoms the smaller the amount of the anneal-induced structural relaxation.

5. Activation energy for enthalpy relaxation $Q_m(T_m)$

The activation energy for structural relaxation can be evaluated from the change in the peak temperature (T_m) of the relaxation curve either by isothermal annealing or continuous heating. If the $\Delta C_{p,endo}$ peak at T_m is associated with a single relaxation entity, an apparent activation energy for enthalpy relaxation, Q_m, of $(Fe\text{-}Ni)_{83}P_{17}$ and $(Fe\text{-}Ni)_{83}B_{17}$ amorphous alloys can be obtained from isothermal annealing data of Figs. 1 to 4 by use of the following relation[40],

$$Q_m(T_m)/k_B = d\ell nt_a^*/d(1/T_a), \qquad (4)$$

where t_a^* is the annealing time for the appearance of $\Delta C_{p,max}$ at T_m and k_B is Boltzmann's constant. As an example, Fig. 17 shows the log t_a versus $1/T_a$ relation for the first stage (open circles) and the second stage (solid circles) for $(Fe_{0.5}Ni_{0.5})_{83}P_{17}$ amorphous samples. A rather good linear relation for each peak, indicating the satisfac-

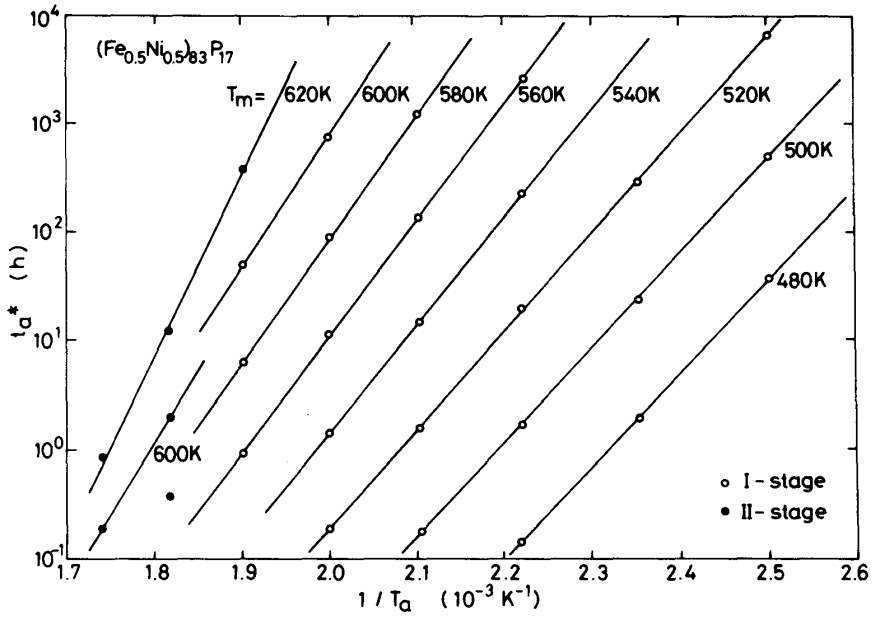

Fig. 17 The annealing time, t_a^*, for the appearance of the ΔC_p peak at T_m as a function of the inverse of the annealing temperature $1/T_a$ for an amorphous $(Fe_{0.5}Ni_{0.5})_{83}P_{17}$ alloy.

tion of an Arrhenius temperature dependence, is seen. As plotted in Fig. 18, $Q_m(T_m)$ of the Fe-Ni-P alloy is not constant and increases with increasing T_m from 1.7 eV at T_m = 475 K to 2.5 eV at T_m = 600 K for the first stage peak and from 2.6 eV at 600 K to 5.0 eV at 650 K for the second stage peak. Similarly, the $Q_m(T_m)$ of $(Fe_{0.5}Ni_{0.5})_{83}B_{17}$ alloy tends to increase with T_m from 1.8 eV at 560 K to 2.0 eV at 620 K.

Alternatively, $Q_m(T_m)$ was evaluated from the shift in the $\Delta C_{p,endo}$ spectrum with scanning rate, α, from equation (5) [41,42],

$$Q_m(T_m)/k_B \simeq \frac{d\ell n(T_m^2/\alpha)}{d(1/T_m)} = -2T_m - \frac{d\ell n\ \alpha}{d(1/T_m)}$$

$$\simeq \frac{d\ell n\ \alpha}{d(1/T_m)}\ , \qquad (5)$$

where $T << Q_m/k_B$. The Q_m values thus evaluated are nearly equal to those obtained from the isothermal data as seen in Fig. 18.

The observed Q_m increases rather drastically by the change of the first-stage peak to the second-stage peak. The relatively small $Q_m(T_m)$ values in the first stage reflect the occurrence of local and/or medium range structural relaxation while the large $Q_m(T_m)$ values in the second stage show cooperative structural relaxation.

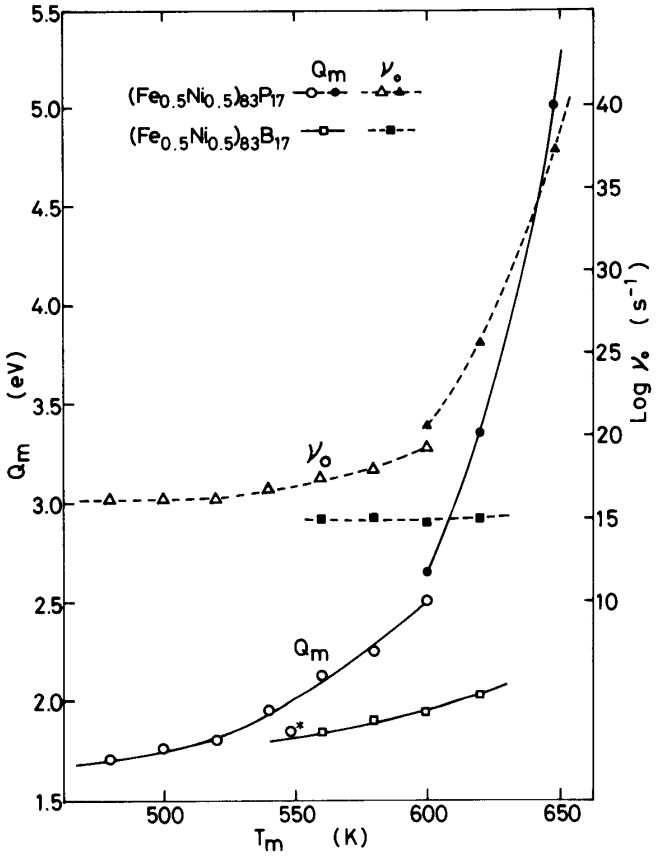

Fig. 18
The activation energy spectrum, $Q_m(T_m)$, and the frequency factor, $\nu_0(T_m)$, as a function of T_m for amorphous $(Fe_{0.5}Ni_{0.5})_{83}P_{17}$ and $(Fe_{0.5}Ni_{0.5})_{83}B_{17}$ alloys.

The activation energy Q_m has the following relation to the frequency factor ν_0 and T_m if a first order rate reaction process for the enthalpy relaxation is assumed;

$$Q_m = k_B T_a \ell n \nu_0 t_a^* = k_B T_m \ell n \nu_0 \tau^* = Q_m(T_m). \quad (6)$$

Here τ^* is the relaxation time at T_g and is related to the scanning rate $\alpha = 2/3$ Ks^{-1} such that $\tau^* = k_B T_m^2/Q_m \simeq 30$ s[43]. The frequency factor $\nu_0(T_m)$ calculated from equation (6) is plotted in Fig. 18. The ν_0 of $(Fe_{0.5}Ni_{0.5})_{83}P_{17}$ alloy increases with T_m from $\simeq 10^{16}$ s^{-1} at 475 K to $\simeq 10^{19}$ s^{-1} at 600 K for the first stage reaction and from $\simeq 10^{20}$ s^{-1} at 600 K to $\simeq 10^{37}$ s^{-1} at 650 K for the second stage reaction, while there is no appreciable change in ν_0 value of $(Fe_{0.5}Ni_{0.5})_{83}B_{17}$ alloy as a function of T_m. These ν_0 values are somewhat higher than Debye frequency $\nu_D \simeq 10^{13} \sim 10^{14}$ s^{-1} for the first stage relaxation and much higher for the second stage relaxation.

IV. Discussion

1. Anneal-induced relaxation spectra

In a previous section, the activation energy for enthalpy relaxation was found to exhibit a broad two-stage distribution against T_m. Based on Primak's theory[44] on the kinetics of processes distributed in activation energy, the enthalpy relaxation spectrum as a function of T_m has been evaluated by Chen[36]. Accordingly, the relaxation spectrum $\Delta C_{p,endo}(T)$ is evaluated from equation (7).

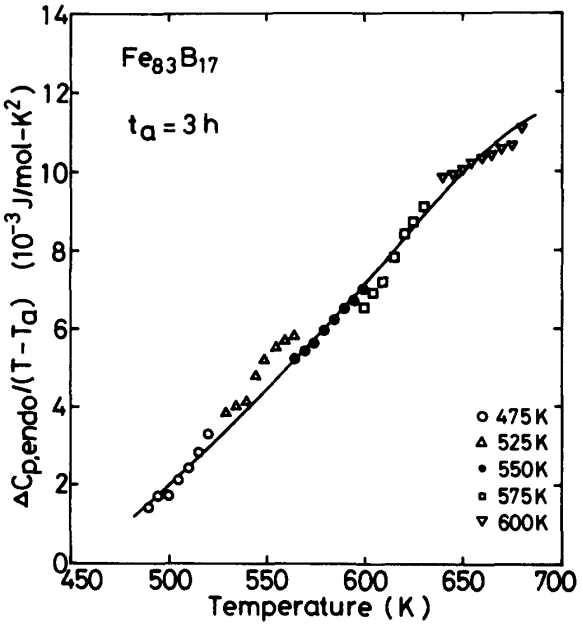

Fig. 19

The relaxation entity spectra, $N_0(T) \simeq \Delta C_{p,endo}(T)/(T - T_a)$ for an amorphous $Fe_{83}B_{17}$ alloy as a function of temperature.

$$\Delta C_{p,endo}(T) = N_0(T)\gamma(T), \qquad (7)$$

where $N_0(T)$ is the distribution of the relaxation entity, and $\gamma(T)$ is the coupling strength contributing to the specific heat $\Delta C_{p,endo}$. As $\gamma(T) \propto (T - T_a)$, equation (8) reduces to

$$N_0(T) \propto \Delta C_{p,endo}(T)/(T - T_a). \qquad (8)$$

$N_0(T)$ values evaluated from the data of $\Delta C_{p,endo}(T)$ are plotted in Fig. 19 for $Fe_{83}B_{17}$ and in Fig. 20 for $(Fe_{0.75}Ni_{0.25})_{83}P_{17}$, $(Fe_{0.5}Ni_{0.5})_{83}P_{17}$ and $(Fe_{0.25}Ni_{0.75})_{83}P_{17}$. It is seen that $N_0(T)$ shows a single maximum near T_g for $Fe_{83}B_{17}$ and two separatable maxima which peak respectively at 490 - 520 K and T_g for $(Fe_{1-x}Ni_x)_{83}P_{17}$ (x= 0.25, 0.50, 0.75). Thus the N_0 - T curves reproduce fairly well the actually measured distribution of the maximum $\Delta C_{p,endo}$ as a function of T_a shown in Figs. 5, 10, 11 and 14. The good reproducibility enables us to conclude clearly that the relaxation entity distributes over one stage against T_a and t_a for $Fe_{83}B_{17}$ alloy and over two stages for $(Fe\text{-}Ni)_{83}P_{17}$ alloys. Judging from the result that T_a dependence of the $\gamma(T)$ and the relatively large frequency factor $\nu_0 > \nu_D$ are similar to the relaxation behavior commonly observed for anneal at temperatures just below T_g, the single stage relaxation spectrum for the

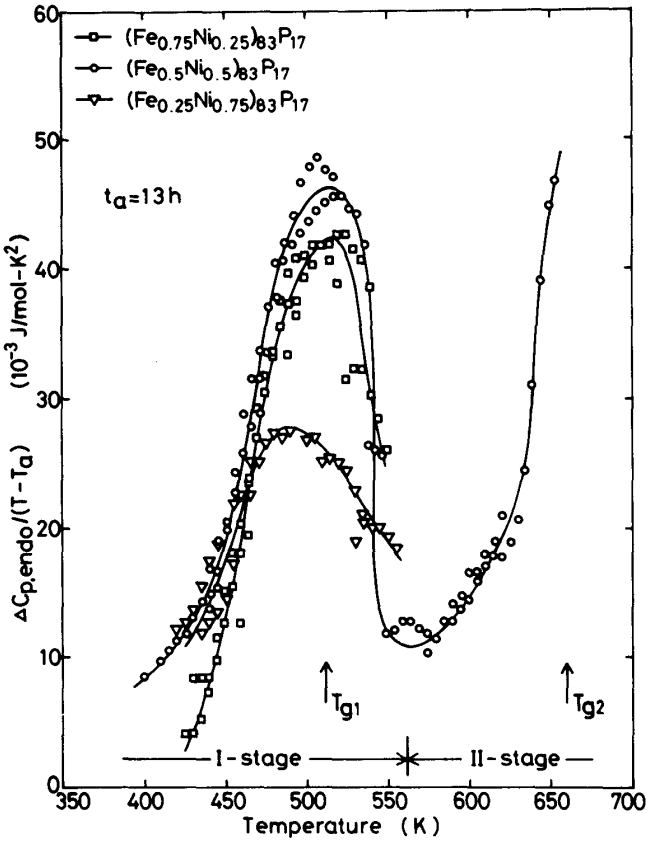

Fig. 20

The relaxation entity spectra, $N_0(T) \simeq \Delta C_{p,endo}(T)/(T - T_a)$ for amorphous $(Fe_{1-x}Ni_x)_{83}P_{17}$ (x= 0.25, 0.50, 0.75) alloys as a function of temperature.

Fe-B alloy is therefore thought to be attributed to a distribution of one kind of glass transition (T_g) with an apparent activation energy Q_m. Similarly, each spectrum of the first- and the second-stage relaxations for the Fe-Ni-P alloys is attributed phenomenologically to a distribution of two kinds of characteristic glass transitions (T_{g1} and T_{g2}) with an individual apparent activation energy Q_1 and Q_2.

2. Interpretation of the single-stage endothermic reaction of Fe-B binary alloy

It has been recently proposed[36,45,46] that a supercooled liquid structure near T_g is inhomogeneous and consists of liquid-like regions of large free volume or high local free energy and solid-like regions with small free volume or low local free energy. The resulting amorphous solid prepared by melt-quenching contains a large number of liquid-like regions with unrelaxed atomic configuration which are isolated from each other embedded in the solid-like matrix. The inhomogeneity in the Fe-B amorphous alloy is thought to arise from fluctuations in concentration and density. When the amorphous solid is annealed at T_a for t_a, parts of the liquid-like regions undergo configurational changes to a more relaxed state in an independent and non-cooperative manner. However, the local structural relaxation in a cluster involving several atoms can be cooperative and the size of this cluster has been estimated to be less than 1-2 nm. Each liquid-like region, m, manifests a liquid-amorphous transition at $T_{g,m}$ which depends on its atomic configuration state. When an amorphous alloy is annealed at temperatures well below T_g, the regions with characteristic relaxation times, τ_m, given by equation (9), being shorter than the duration of the annealing time (t_a), ($\tau_m < t_a$) undergo local relaxation towards the local equilibrium states at T_a.

$$\tau_m \simeq \tau_{mea} \exp[-\frac{Q_m}{k_B}(1/T_a - 1/T_{g,m})] \qquad (9)$$

Here τ_{mea} is the time constant of measurement. Each local relaxation contributes to the enthalpy relaxation in proportion to $(T_a - T_{g,m})$. Upon heating the annealed sample, each region, m, recovers the initial structure (so-called "reversion") and contributes to an excess endothermic specific heat as the local amorphous-liquid transition occurs at or slightly above $T_{g,m}$. Thus the peak temperature of the $\Delta C_{p,endo}$ evolves in a continuous manner against the logarithm of t_a with intensity proportional to $(T_{g,m} - T_a)N_0(T_{g,m})$. Therefore, the reason why the endothermic reaction for the Fe-B binary amorphous alloys evolves over a single stage is concluded to be due to a monotonous increase of $N_0(T_{g,m})$ for the binary amorphous alloys as a function of temperature as is evidenced in Fig. 19.

3. Interpretation of the two-stage endothermic reaction of Fe-Ni-P and Fe-Ni-B alloys

The above-mentioned relaxation mechanism deals with a single atomic interacting system of metal and metalloid and gives a single broad distribution of relaxation times (or glass transitions). In many ternary and quaternary amorphous alloys, there exist two types of short-range ordering, e.g., metal-metal and metal-metalloid type, and the latter shows much stronger ordering than the former. This is manifested by a drastic increase in T_g with the addition of metalloid elements in metal-metalloid amorphous alloys. We thus expect higher mobility or faster relaxation for the metal-metal than for the metal-metalloid pairs.

Taking into account two types of atomic pairs existing in the Fe-Ni-P and Fe-Ni-B amorphous alloys, we propose the existence of two distributions of glass transitions centering at T_{g1} and T_{g2} respectively (see Fig. 20). T_{g1} corresponds to glass transition arising from the metal atoms and T_{g2} to that from metal-metalloid atoms. The relaxation spectra are seen to be asymmetric with a long tail in the short time. The metal-metal pairs are more less confined in the skeleton of metal-metalloid pairs. The local range rearrangement of metal atoms with a weak bonding occurs in the low temperature range near T_{g1}, while the atomic regroupings involving metal-metalloid atoms take place at higher temperatures near T_{g2}. That is, the marked difference in bonding force among the constituent elements is the main reason for the appearance of the two-stage enthalpy relaxation which is evidenced from the data (Fig. 20) showing the two-stage distribution of the N_0 - T curve for the $(Fe\text{-}Ni)_{83}P_{17}$ alloys. This new viewpoint is substantiated from the present results that the low temperature endothermic peak is barely detectable in Fe-B binary alloys and the alloying of metallic components leads to an increase in $\Delta C_{p,endo}$ values as well as $\Delta C_{p,exo}$ at the first stage. In addition, the reason why the magnitude of the endothermic peak for $(Fe_{0.5}Ni_{0.5})_{100-x}B_x$ (x= 17, 20, 25) amorphous alloys decreases with increasing boron content is thought to originate from an enhancement of the difficulty in atomic rearrangement during annealing (an increase in relaxation times) due to the increase in the number of iron-boron and nickel-boron pairs with strong bonding force and the decrease in that of iron-iron, iron-nickel and nickel-nickel pairs with weak bonding force. The occurrence of the minimum phenomenon in the $\Delta C_{p,endo}$ and $\Delta H_{\sigma,endo}$ spectra shown in Figs. 3 to 14 can be explained by taking into consideration of the two distributions of glass transitions.

4. Possible process of structural relaxation

From the above-described results and discussion, we propose a possible structural relaxation process shown in Fig. 21. The structural relaxation of an amorphous phase is divided into irreversible and reversible processes which consist of two stages; the first stage is the short-range rearrangement which occurs by the interaction involving only metal atoms and the second stage is a relatively long-range atomic regrouping which occurs by interaction between metal and metalloid. The two-stage structural relaxations lead to the annihilation of various kinds of quenched-in "defects" and the enhancement of topological and chemical short-range ordering for the irreversible process, and to the enhancement of compositional (chemical) short-range ordering for the reversible process. It is quite encouraging that the newly proposed process can explain many of the phenomenological features observed for low- and high-temperature anneals for a number of amorphous alloys such as Fe-P, Fe-B, Ni-P, Ni-B, Fe-Ni-P, Fe-Ni-B, Fe-Si-B[30], Co-Si-B[30], Ni-Si-B[30], Fe-Ni-Si-B[30], Fe-Co-Si-B[30], Co-Ni-Si-B[30] and Pd-Ni-Si[47]. Since the relaxation due to the interaction of metal-metal atoms can be faster by a factor of many orders of magnitude than the cooperative relaxation process due to metal-metalloid atoms responsible for the commonly observed glass transition, the concept of the distribution of the glass transition due to metal-metal atoms with short relaxation time is significant and valuable in the understanding of the stability of amorphous alloys at low temperatures.

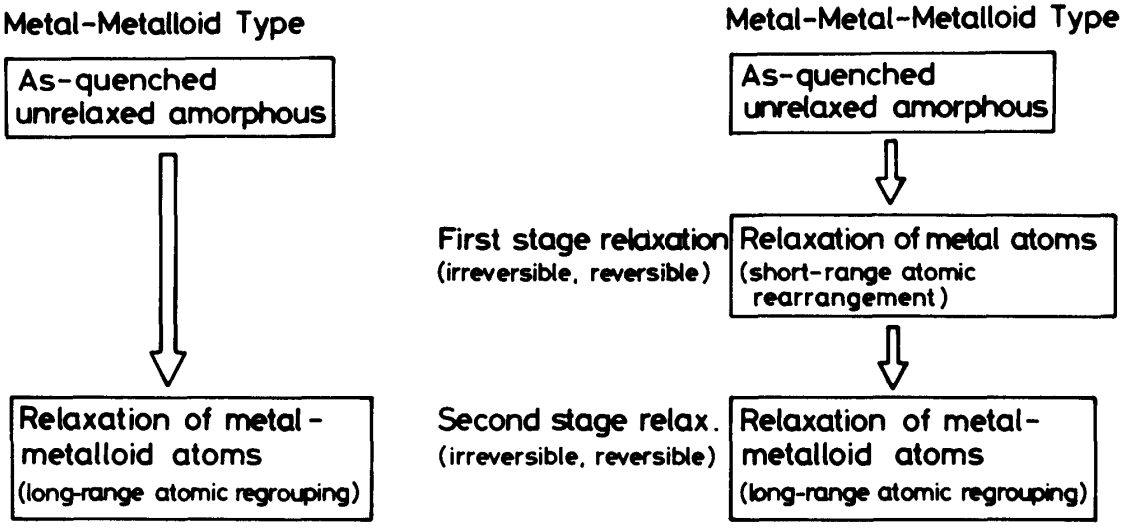

Fig. 21 Irreversible and reversible structural relaxation processes of metal-metalloid and metal-metal-metalloid amorphous alloys.

Finally, in order to appeal the universality of the present concept on the structural relaxation of amorphous alloys, it is worthy to note that the anneal-induced relaxation of metal-metal type amorphous alloys such as Cu-Zr, Ni-Zr, Cu-Zr-Fe and Cu-Zr-Ni etc. has also been demonstrated[32] to occur through the similar process as that shown in Fig. 21. That is, the structural relaxation of Cu-Zr and Ni-Zr binary amorphous alloys occurs at a single stage with a peak at $\simeq T_g$, while it for Cu-Zr-Fe and Cu-Zr-Ni ternary amorphous alloys can be separated into two stages; a low temperature (first stage) peak at about T_g - 150 K and a high temperature (second stage) peak at a temperature slightly below T_g. From the result that the addition of iron or nickel to Cu-Zr alloys causes the two-stage splitting of the structural relaxation, it has been proposed[32] that the low temperature relaxation peak is attributed to the short-range rearrangement of copper and iron or nickel atoms with weak bonding nature and the high temperature relaxation to the long-range cooperative regrouping of zirconium and copper, iron or nickel atoms which are composed of the skeleton structure in the metal-metal amorphous alloys.

V. Summary

In order to clarify the compositional effects on the two-stage enthalpy relaxation phenomenon found previously by the present authors, structural relaxation behavior of the pre-annealed samples over a wide temperature range from well below the glass transition temperature T_g to T_g was investigated calorimetrically for amorphous $(Fe_{1-x}Ni_x)_{83}P_{17}$, $(Fe_{1-x}Ni_x)_{83}B_{17}$ (x=0, 0.25, 0.50, 0.75, 1.0), $(Fe_{0.5}Ni_{0.5})_{100-y}P_y$, $(Fe_{0.5}Ni_{0.5})_{100-y}B_y$ (y=15, 17, 20, 25) and $(Fe_{0.33}Ni_{0.33}Co_{0.34})_{83}P_{17}$ alloys. The results obtained are summarized as follows:

1. Upon heating the annealed samples, an excess endothermic reaction (enthalpy relaxation) occurs above T_a followed by a broad exothermic reaction. The peak temperature of the endothermic reaction, T_m, increases in a continuous manner with ℓnt_a.

2. The change in the magnitude of the $\Delta C_{p,endo}$ peak with T_a for the Fe-P, Fe-B, Ni-P and Ni-B alloys occurs at a single stage with a peak at $\simeq T_g$. On the other hand, for the Fe-Ni-P and Fe-Ni-B ternary alloys, it can be separated into two stages; a low-temperature (first-stage) peak at about T_g - 200 K and a high-temperature (second-stage) peak at a temperature slightly below T_g. The activation energy increases with increasing T_m from 1.7 eV at T_m = 475 K to 2.5 eV at T_m = 600 K for $(Fe_{0.5}Ni_{0.5})_{83}P_{17}$ and from 1.8 eV at 560 K to 2.0 eV at 620 K for $(Fe_{0.5}Ni_{0.5})_{83}B_{17}$ for the first-stage ($T_a < T_g$ - 120 K) relaxation

and from 2.6 eV at 600 K to 5.0 eV at 650 K for the Fe-Ni-P for the second-stage (T_g - 120 K < T_a < T_g) relaxation.

3. From the result that the addition of other metallic elements causes the appearance of another low-temperature peak in the $\Delta C_{p,endo}$ - T_a relation, the endothermic relation has been interpreted to be due to the short-range rearrangement of metal-metal atoms with weak bonding nature for the first-stage peak and to the long-range cooperative rearrangements of metal-metalloid atoms, which are composed of the skeleton structure in metal-metalloid type amorphous alloys, for the second-stage peak. By an endothermic reaction each region recovers from a relaxed configuration caused by annealing to an unrelaxed initial structure. The occurrence of the two-stage reversible enthalpy relaxation for the amorphous alloys containing more than two metallic elements appears to originate from a dual distribution of glass transitions centered around T_{g1} and T_{g2} which arise respectively from metal-metal atoms and metal-metalloid atoms.

4. A possible structural relaxation mechanism leading to the annihilation of various kinds of frozen-in "defects" and the development of topological and compositional short-range ordering has been proposed; as-quenched unrelaxed amorphous → irreversible and reversible relaxation of metal atoms in a short range → irreversible and reversible relaxation of metal-metalloid pair atoms over a long range. The newly proposed structural relaxation mechanism is believed to explain fairly well many of phenomenological features in the structural relaxation observed for the anneals in the whole temeprature below T_g.

References

(1) H.S. Chen, R.C. Sherwood, H.J. Leamy and E.M. Gyorgy, IEEE Trans., MAG-12 (1976), 933.

(2) T. Egami, Mater. Res. Bull., 13 (1978), 557.

(3) H.S. Chen, J. Appl. Phys., 49 (1978), 4595.

(4) A.L. Greer and J.A. Leake, J. Non-Cryst. Solids, 38/39 (1980), 379.

(5) A.J. Drehman and W.L. Johnson, Phys. Stat. Solids, (a) 52 (1979), 499.

(6) A. Ravex, J.C. Lasjaunias and O. Bethoux, Physica, 107B (1981), 397.

(7) C.C. Koch, D.M. Kroeger, J.S. Lin, J.O. Scarbrough, W.L. Johnson and A.C. Anderson, Phys. Rev., 27 (1983), 1586.

(8) A. Inoue, S. Okamoto, N. Toyota, T. Fukase, K. Matsuzaki and T. Masumoto, J. Mater. Sci., 19 (1984), 2719.

(9) A. Inoue, K. Matsuzaki, N. Toyota, H.S. Chen, T. Masumoto and T. Fukase, J. Mater. Sci., 20 (1985), in press.
(10) M. Balanzat, Scripta Met., 14 (1980), 173.
(11) M. Balanzat, C. Maivy and J. Hillaret, J. Phys., C-8 (1980), 871.
(12) J. Hillairet, E. Balanzat, N.E. Derradji and A. Chamberod, J. Non-Cryst. Solids, 61/62 (1984), 781.
(13) T. Komatsu, R. Yokota, T. Shindo and K. Matsushita, J. Non-Cryst. Solids, 65 (1984), 63.
(14) H.S. Chen, J. Appl. Phys., 49 (1978), 3289.
(15) A. Kursumovic, M.G. Scott, E. Grit and R.W. Cahn, Scripta Met., 14 (1980), 1303.
(16) B. Fogarassy, A. Bohonyei, A. Cziraki, I. Szabo, G.Y. Faigel, L. Granasy, T. Kemeny and I. Vincze, J. Non-Cryst. Solids, 61/62 (1984), 907.
(17) H.S. Chen, H.J. Leamy and M. Barmatz, J. Non-Cryst. Solids, 5 (1971), 448.
(18) M. Barmatz and H.S. Chen, Phys. Rev., 139 (1974), 4073.
(19) B.S. Berry and W.C. Pritcher, J. Appl. Phys., 44 (1973), 3122.
(20) T. Soshiroda, M. Koiwa and T. Masumoto, J. Non-Cryst. Solids, 21 (1976), 688.
(21) N. Morito and T. Egami, Acta Met., 32 (1984), 603.
(22) H.S. Chen and N. Morito, Proc. of the 5th Int. Conf. on Rapidly Quenched Metals, September 3-7, 1984, Wurzburg, F.R.G., in press.
(23) H.S. Chen, Mater. Sci. Eng., 26 (1976), 79.
(24) A. Inoue, H.M. Kimura and T. Masumoto, J. Japan Inst. Metals, 42 (1978), 303; Sci. Rep. RITU, A-27 (1979), 159.
(25) H.R. Kimura and D.G. Ast, Proc. of the 4th Int. Conf. on Rapidly Quenched Metals, eds. T. Masumoto and K. Suzuki, Japan Inst. Metals, Sendai (1982), 475.
(26) K.E. Heusler and D. Huerta, Int. Congress on Metallic Corrosion, National Research Council Canada, Toronto (1984), 222.
(27) Y. Masumoto, A. Inoue, A. Kawashima, K. Hashimoto and T. Masumoto, J. Mater. Sci., to be submitted.
(28) H.S. Chen, Amorphous Metallic Alloys, ed. F.E. Luborsky, Butterworths, London (1983), 169.
(29) H.S. Chen, Proc. of the 5th Int. Conf. on Rapidly Quenched Metals, September 3-7, 1984, Wurzburg, F.R.G., in press.
(30) A. Inoue, T. Masumoto and H.S. Chen, J. Mater. Sci., 20 (1985), in press.
(31) A. Inoue, T. Masumoto and H.S. Chen, J. Mater. Sci., 20 (1985), in press.

(32) A. Inoue, T. Masumoto and H.S. Chen, J. Mater. Sci., 20 (1985), in press.
(33) A.J. Kavacs, Fotchr. Hochpolym-Forsch, 3 (1963), 394.
(34) H.S. Chen, J. Appl. Phys., 49 (1978), 4595.
(35) R.O. Suzuki and P.H. Shingu, J. Non-Cryst. Solids, 61/62 (1984), 1003.
(36) H.S. Chen, J. Non-Cryst. Solids, 46 (1981), 289.
(37) L.A. Davis, R. Ray, C.P. Chou and R.C. O'Hanley, Scripta Met., 10 (1976), 541.
(38) L.A. Davis, Metallic Glasses, ASM, Metals Park, Ohio (1978), 191.
(39) A. Inoue, H.S. Chen, J.T. Krause, T. Masumoto and M. Hagiwara, Sci. Rep. RITU, A-31 (1983), 124.
(40) H.S. Chen, J. Non-Cryst. Solids, 27 (1978), 257.
(41) T. Ozawa, Polymer, 12 (1971), 51.
(42) C. Antonione, L. Battezzati, A. Lucci, G. Riontino and G. Venturello, Scripta Met., 12 (1978), 1011.
(43) H.S. Chen, Sci. Rep. RITU, A-27 (1979), 97.
(44) W. Primak, Phys. Rev., 100 (1955), 1677.
(45) M.H. Cohen and G.S. Grest, Phys. Rev., B20 (1979), 1077.
(46) M. Cyat, J. Phys., C-8 (1980), 107.
(47) A. Inoue, T. Masumoto and H.S. Chen, unpublished research, 1984.